Cellular and Molecular Biology
E-ISSN : 1165-158X / P-ISSN : 0145-5680
www.cellmolbiol.org

The potential role of exosome-derived mesenchymal stem cells and *Balanites aegyptiaca* in diabetic nephropathy amelioration in rats

Nashwa Barakat[1], Mohamed Ali[2], Aml Nassr[2*], Faten Zahran[2]

[1] Urology and Nephrology Center, Mansoura University, Mansoura, Egypt
[2] Biochemistry Division, Chemistry Department, Faculty of Science, Zagazig University, Zagazig, Egypt

ARTICLE INFO

Original paper

Article history:
Received: November 24, 2022
Accepted: February 26, 2023
Published: February 28, 2023

Keywords:

Exosomes, characterization, mesenchymal stem cells isolation, Balanites aegyptiaca

ABSTRACT

The utilization of mesenchymal stem cell (MSC)-derived exosomes, which include numerous growth factors, cytokines, and microRNAs, is the primary aspect of the novel MSC activity models. The current research aims to: (i) identify the morphology of exosomes; (ii) determine exosomes secreted into MSCs conditioned cell culture medium; and (iii) perform a comprehensive characterization of isolated exosomes and elucidate their protective role in the diabetic nephropathy animal model. Ultracentrifugation was performed by utilizing the culture supernatant of MSCs. Transmission electron microscopy, nanoparticle tracking analysis, as well as Western blot, were utilized for isolated exosome characterization. The purified exosomes were used for *in vivo* implantation in a diabetic nephropathy animal model. The present research was carried out on 70 adult male albino rats weighing 180 to 200 grams. Rats were classified into seven groups: Group I: negative control group; Group II: diabetic nephropathy group; Group III: *Balanites* therapeutic group; Group IV: *Balanites* + MSCs therapeutic group; Group V: *Balanites* + exosome therapeutic group; Group VI: MSCs therapeutic group; and Group VII: exosome therapeutic group. By the end of the study period, total antioxidant capacity (TAC), malondialdehyde (MDA), and the histology of pancreatic tissue were assessed. Isolated exosomes with sizes ranging from 30 to 150 nm demonstrated the typical cup-shaped morphology. Additionally, exosome criteria were demonstrated by the exosome surface proteins CD81 and CD63, which were expressed by exosome marker proteins. Treatment with exosomes along with *Balanites* induced a significant reduction in pancreatic MDA with a substantial elevation in pancreatic TAC. Furthermore, treatment with exosomes and *Balanites* demonstrated normal pancreatic parenchyma and pancreatic lobules with normal pancreatic acini and acinar cells. These findings strongly suggest that ultracentrifugation is the most efficient tool for isolating exosomes. Also, these findings demonstrated that *Balanites* and exosomes had synergistic effects on one another, with more potent renoprotective activities in rats.

Doi: http://dx.doi.org/10.14715/cmb/2023.69.2.7

Introduction

Cellular exosomes are a particular type of extracellular vesicle that cells secrete into the extracellular environment via the endocytic pathway (1). The exosomes are released during endosome-plasma membrane fusion. An endosome membrane invagination produces them to generate vesicles located within the endosome's lumen or multivesicular bodies (MVBs) (2). Exosomes frequently contain plasma membrane proteins, cell cytosol, lipids, metabolites, and nucleic acids such as miRNA, mRNA, non-coding RNA, and DNA (3). They are hypothesized to be involved in many processes, including cell-cell information exchange, coagulation, antigen presentation, and protein and nucleic acid transfer (4). When various types of cells are grown in a culture medium, they release membrane-bound vesicles termed extracellular vesicles (EVs) (5), containing vesicles of various sources, biogenesis, composition, and sizes. Apoptotic bodies (1,000-5,000 nm), microvesicles (100-1,000 nm), and exosomes (30-100 nm) that are secreted by apoptotic cells are the three broad categories to which EVs belong (6). Exosomes are vesicles with surrounding lipid bilayers having a 1.10–1.20 g/ml density. They are released following MVB fusion with the plasma membrane, and they include various membrane-associated proteins, including tetraspanins (e.g., CD82, CD81, CD9, and CD63), proteins implicated in the biosynthesis of MVB (TSG101 and Alix), MHC-I and MCH-II, GTPases, and heat-shock proteins (HSP) (7). The tetraspanin protein family members CD81, CD63, and CD9, are the most prevalent exosome surface markers. These proteins assemble tetraspanin-rich microdomains to mediate exosome secretion and assist in exosome organization (8).

The physiological function of exosomes is poorly understood. In addition, they are significant components in various cell types' conditioned cell culture medium, including MSCs. Initially, it was believed that the primary function of exosomes was to transport and eliminate extra protein and other nonfunctional cellular molecules (9). In the cardiac ischemia/reperfusion injury animal model, MSC-derived exosomes were initially studied (10). Multiple studies revealed the capacity of exosomes produced from MSCs to renew and repair tissue, their potential for preventing apoptotic and reducing inflammation, and their involvement in cardiac remodeling and regeneration processes (11). Exosome isolation and identification pave the

* Corresponding author. Email: amal.nasr@zu.edu.eg

way for cell-free therapy, which may help overcome cell therapy limitations like immunological incompatibility, prolonged waiting periods, and high prices associated with manufacturing biological substances (12). Exosome isolation aims to obtain a pure sample of exosomes to study their action mechanisms and potential biomedical applications. Numerous additional methods have been developed. Several scientists managed to isolate exosomes utilizing affinity capture, polymer-based precipitation, ultrafiltration, chromatography, and ultracentrifugation. Exosome isolation occurs using various methods, depending on their source, but ultracentrifugation is the most common. This technique is effective at pelleting molecules such as aggregates, extravesicular protein complexes, and lipoproteins. However, it is a time-consuming procedure with several phases and expensive equipment (13). This work aims to characterize and identify exosomes extracted from the MSCs' cell culture supernatant, in addition to identifying and counting the number of exosomes generated.

Materials and Methods

Preparation of MSCs derived exosomes

Exosomes generated from MSCs were isolated using the supernatants of MSC-conditioned media. MSCs derived from rat bone marrow were prepared at the Faculty of Medicine's Medical Experimental Research Center (MERC), Mansoura University, Egypt. In Dulbecco's Modified Eagle Medium (DMEM), lacking fetal bovine serum and with 0.5% human serum albumin (Sigma-Aldrich), MSCs were cultivated overnight. Trypan blue exclusion revealed that cell viability (for cells-cultured overnight) would surpass 99%. For seven days, a cell density of 4,000 cells per cm^2 was used for cell plating. On day seven, cells were trypsinized using 0.25% trypsin in one mmol per liter EDTA at 37°C for 5 min, counted, and then replated in growth media at 2000 cells per cm^2 for an additional 7-day period (end of passage 1). The growth was maintained until the third passage (14). A collection of the conditioned media was formed and kept at -80°C.

Isolation of MSC-derived exosomes

MSCs were cultured in a normal growth medium until they reached 80% confluence. A serum-free medium was substituted for the medium. For removing any remaining cells, the media for cell culture was collected after 48 hours and then centrifuged at 4°C for ten minutes at 300 xg, followed by 2000 xg for 10 minutes, and then 10000 xg for 30 minutes. Twenty ml of supernatant was centrifuged at 100,000 xg (Sorvall SureSpin 630) for 70 minutes at 4°C to isolate exosomes. This resulting pellet was rinsed using an equal volume of ice-cold PBS before being centrifuged for 70 minutes at 100,000 xg 4°C. The EVs were subsequently contained in the pellet. The exosome-containing pellet was suspended in phosphate buffer saline (50 to 100 µl) (15).

MSC-derived exosomes characterization

Transmission electron microscopy (TEM)

Paraformaldehyde at a concentration of 2% was used to fix exosome samples. On EM grids with Formvar carbon coating, five µl of each sample were applied, and they were left to adsorb for 20 minutes at room temperature. Grids underwent two rinses in water for five minutes before contrast (negatively) staining EVs with 1% phosphotungstic acid for thirty seconds after samples were fixed with glutaraldehyde (1%). The removal of grids was performed using stainless steel loops. In addition, the filter paper was used to absorb any extra liquid. The produced exosomes were observed after drying using a transmission electron microscope (Hitachi H-7650, Hitachi, Tokyo, Japan) with an 80-kilovolt acceleration voltage and magnifications ranging from 20,000X to 100,000X to determine the particles' size (16).

Nanoparticle tracking analysis

A 1:10 dilution of exosomes in phosphate buffer saline was used for NanoSight LM20 nanoparticle tracking analysis (NTA) (NanoSight, Malvern Panalytical Ltd, Malvern, UK). Each particle's Brownian motion was followed over frames, and the Stokes-Einstein equation was used to determine its size (17).

Protein quantification in the isolated exosomes

PBS was used to extract and re-dissolve the pellet. The BCA Protein Assay Kit (Boster Biological Technology, Pleasanton, CA, USA, Catalog # AR0146- 500) was used to assess the protein content of the extracted exosome fraction using the standard "bovine serum albumin" per the manufacturer's guidelines.

Western blotting

Exosomes were lysed in RIPA buffer using protease inhibitors and 1 mM phenylmethylsulfonyl fluoride. Exosomal lysates in equal volumes (50 µL) were subjected to non-reducing 12.5% SDS-PAGE for CD63 and CD81 and subsequently transferred utilizing a wet transfer system (Bio-Rad Laboratories, Hercules, CA, USA) on a PVDF membrane (MDI Membrane Technologies, Harrisburg, PA, USA). After blocking, in 1 TBS-T solution (1:5000; Abcam, Cambridge, MA, USA) containing 5 percent nonfat skim milk, the membrane was incubated with the CD63 primary antibody. The antibodies utilized were CD63 (Biolegend, Cat. No. 0353007) and polyclonal sheep IgG anti-rabbit CD81 (Biolegend, Cat. No. 0349509) with antigen affinity purification, as well as beta-actin. They were incubated at 4°C overnight. After being washed, the blot was incubated with a secondary antibody conjugated to horseradish peroxidase (HRP), and it was then developed utilizing an ECL imager (Invitrogen, a brand of Thermo Fisher Scientific).

Exosome labeling with PKH26

To label an aliquot of frozen EV, Sigma-PKH26 Aldrich's Fluorescent Cell Linker Kits were utilized based on the manufacturer's instructions. A frozen aliquot of EV was resuspended in phosphate-buffered saline (1ml). PKH26 was utilized to determine the localization of exosomes in kidney tissue (Sigma-Aldrich, St. Louis, MO, USA). The exosome pellet was diluted to a volume of 1 ml using the kit solution from the PKH-26 kit. Afterward, 2µ of the fluorochrome was added to this suspension. This suspension was then incubated for 15 minutes at 38.5°C. After adding 7 ml of serum-free HG-DMEM. The suspension was ultracentrifuged again for one hour at 100,000 g and 4°C. In order to inject the final pellet into an experimentally induced rat later, it was instantly resuspended in

HG-DMEM and kept at -80°C (18).

Preparation of *Balanites aegyptiaca* fruits aqueous extract

The coat epicarp of collected *Balanites aegyptiaca* fruits was carefully removed manually, and also the fruit's mesocarp was subsequently peeled with a cleaned, dried knife. The fleshy outer layer named the mesocarp then detached from the seeds. The dried mesocarp in the air was then ground with a coffee grinder in the laboratory. After that, it was kept in the refrigerator in a dry plastic container even after it was needed. Following the removal of seeds, one kilogram of dried fruit was submerged in distilled H_2O for 24 hours (200 ml distilled H_2O was used to extract 100-gram powder). This recently made filtrate passed freeze drying (utilizing Labcono, model 18, freeze dryer) to produce a thick dark brown extract. Prepared aqueous *Balanites aegyptiaca* fruit extract was injected orally by an oral gastric tube every day for four weeks at a dose of 80 mg/kg b. wt. (19).

Experimental animals

Seventy male adult albino rats were put in the experimental animal house of Zagazig University's Faculty of Science, weighing 180 ± 200 grams. Rats were placed in a controlled setting with a 25°C temperature, 65% relative humidity, and a twelve-hour cycle of light and dark. The adult rats had unlimited access to commercial pellet rat chaw and tap water. The Zagazig University's Ethical Committee approved the handling of animals and study design (ZU-IACUC/1/F/80/2019).

Induction of diabetic nephropathy in rats

Induced diabetic nephropathy was induced intraperitoneally with a single freshly prepared streptozotocin (STZ) injection (60 mg/kg b. wt., STZ) dissolved in (100 mM, pH = 4.5) cold citrate buffer in overnight-fasted adult rats following 15 minutes of intraperitoneal (i.p) nicotinamide injection (120 mg/kg body weight, NIC) dissolved in 0.9% (wt./v) sodium chloride. To prevent hypoglycemia, rats received an overnight 5% glucose solution after one hour of STZ and nicotinamide injection. Fasting blood sugar levels were determined by utilizing a portable glucose meter for 72 hours following injection and on day seven. Diabetic rats had fasting blood sugar levels higher than 250 mg/dl(20). Compared with controls, substantial increases in serum creatinine and urea levels, as well as histological alterations, confirmed nephropathy in male adult albino rats at the end of the sixth week after induction. This study included rats with these significant values (21).

Experimental design

In this experiment, 70 rats were categorized into seven groups, each with ten rats. The groups were categorized as follows:

Group **I**: Negative control; normal rats.

Group **II**: Positive control; diabetic nephropathy group.

Group **III**: *Balanites* treated group; diabetic nephropathy was induced, and rats were treated with the prepared *Balanites aegyptiaca* fruit aqueous extract administered orally by an oral gastric tube at an 80 mg/kg body weight dose every day for four weeks (19).

Group **IV**: *Balanites* + MSCs treated group; diabetic nephropathy was induced in rats, and they received prepared *Balanites aegyptiaca* fruit aqueous extract of (80 mg/kg) orally for four weeks daily (19) and MSCs (1.0×10^4 cell/g) two times every four weeks via the tail vein (22).

Group **V**: *Balanites* + exosomes treated group; diabetic nephropathy was induced in rats, and they received prepared *Balanites aegyptiaca* fruit aqueous extract of (80 mg/kg) orally for four weeks daily (19) and twice exosome injection (100 µg per kg per dose dissolved in 200 µL PBS) (23). The first was administered in the eighth week of the study, while the second was administered after the tenth week(21).

Group **VI**: MSCS treated group; four weeks following STZ injection, DN rats were treated with 1.0×10^4 MSCs per gram b. wt per animal suspended in 200 µL phosphate buffer saline (PBS) two times every four weeks via the tail vein (22).

Group **VII**: Exosome-treated group; rats were induced with diabetic nephropathy and administered twice intravenous injections of exosomes (100 g per kg per dose dissolved in 200 µL phosphate-buffered saline (PBS) intravenously (23). The first was administered in the eighth week of the study, while the second was administered at the end of the tenth week (21).

Tissue sampling

Saline-washed pancreatic tissue was cut into portions and homogenized in 10 mM potassium phosphate buffer (pH = 7.4). The weight ratio of the homogenized tissue to the buffer used was 1:5. The homogenates were centrifuged at 4000 g at 4°C for 10 minutes to collect the supernatant for MDA and TAC measurements, while the remaining was immersed in neutral buffered formalin at 10% for histological analysis.

Biochemical parameters

Determination of oxidative stress and antioxidant biomarkers in pancreatic tissue homogenate

The homogenized pancreatic tissue sample was utilized to determine oxidative stress and antioxidant biomarkers. The MDA level was measured colorimetrically using a commercial kit obtained from Biodiagnostic Company, Egypt, to monitor the extent of lipid peroxidation (24). The total antioxidant capacity was assessed utilizing commercial kits purchased from Biodiagnostic Company, Egypt (25).

Histopathological examination of the pancreas:

After 24 hours of sacrification, pancreatic tissue samples were immediately fixed in neutral buffered formalin at a concentration of 10 percent. Then, 4-µm-thick paraffin slices were prepared using the fixed samples through a processing step. Hematoxylin and eosin (H&E) were used to examine the pancreas structure by staining prepared slices. The slides were then examined using a light microscope (26).

Morphometry

Sections underwent semi-quantitative analysis for the histological assessment of the severity of pancreatic lesions (27); Score 0: normal, score +: mild to normal, score ++: mild (<25% of the total fields analyzed showed changes), score +++: moderate (<50% of the total fields analyzed showed changes), and score ++++: severe (< 75% of the

total fields analyzed showed histopathological changes).

Statistical analysis

Version 25 of the statistical package for social science (SPSS) (28) for Windows was used to code and enter the data. The mean and standard error (SE) were used to express quantitative data. A one-way analysis of variance (one-way ANOVA) was utilized for comparing quantitative data from more than two groups. The significance level was set at a p-value of ≤ 0.05.

Results

Exosome characterization using transmission electron microscopy (TEM)

The ultracentrifugation technique was initially utilized to isolate exosomes from a cell culture medium. Nanovesicles were detected using transmission electron microscopy; however, the sizes of the individual EVs were heterogeneous, with a typical diameter range of 30 to 150 nm, as shown in Figure 1.

Nanoparticle tracking analysis (NTA)

NTA is a technique for examining particles in liquids called nanoparticle tracking analysis that links Brownian motion rate to particle size. The size distribution profile of tiny particles with a diameter of roughly 10-1000 nanometers (nm) in liquid suspension can be determined using NTA. The sharpest size distribution curves for exosomes were 109 ± 1.77, which is consistent with transmission electron microscopy and suggests more uniform preparations, as shown in Figure 2.

Exosome concentration by BCA assay

A BCA protein assay kit was utilized for measuring the quantity of protein in the isolated exosomes, as in Table 1. In addition, the needed exosome concentration for western blot analysis and the dose for *in vivo* investigation were adjusted.

Characterization of exosome by Western blot using exosome–specific surface marker

Immunoblotting with antibodies specific to the exosome surface markers CD63 and CD81 confirmed that the MSC-isolated exosomes were exosomes. Through the production of exosome surface proteins, Western blot analysis demonstrated that the extracted EVs were abundant in exosomal marker proteins, supporting the exosomal criteria. Beta-actin utilizes a housekeeping gene along with CD63 (55 KDa) and CD 81 (23 KDa), as shown in Figure 3.

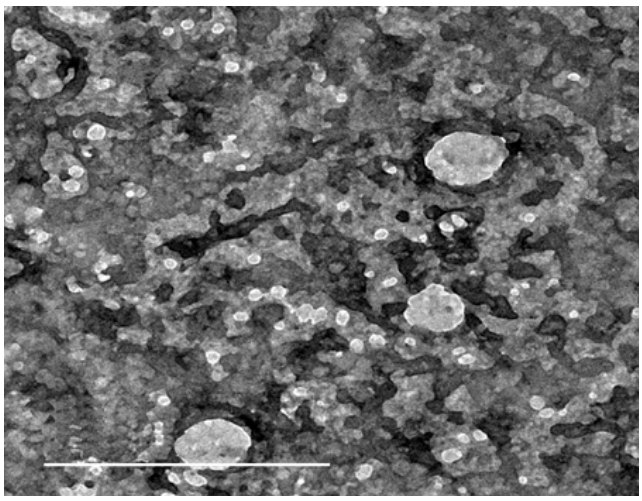

Figure 1. Transmission electron micrograph of isolated exosomes using ultracentrifugation from MSC-conditioned media (Scale Bar = 500 nm).

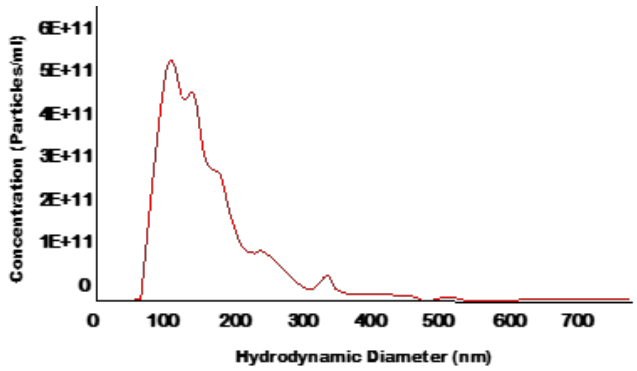

Figure 2. Size analyses of isolated exosomes; nanoparticle tracking analysis of exosomes.

Table 1. Concentration of exosomes expressed by µg/ml isolated from MSCs by BCA assay.

Sample Number	The concentration of exosomes (µg/ml)
1	494.00
2	440.67
3	350.67
4	494.00
5	440.67
6	350.67
Mean	428.44

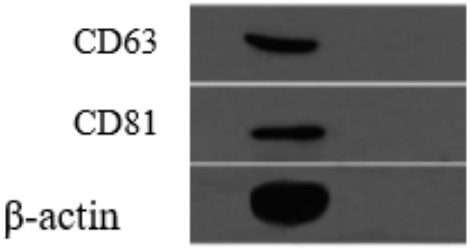

Figure 3. Western blot analysis of exosomes shows the presence of CD 63 and CD 81 proteins.

Exosome labeling and uptake

To examine the capacity of exosomes to enter cells, EVs labeled with PKH26 were incubated for 90 minutes with cells maintained at 4°C or 37°C. Images of MSCs incubated at different temperatures revealed that cells cultured at 37°C had significantly higher fluorescence than those incubated at 4°C, as shown in Figure 4, denoting that EVs penetrated the cells.

Effect of the exosome, MSCs, and *Balanites aegyptiaca* on MDA and TAC in pancreatic tissue

TAC and MDA concentrations in the pancreatic tis-

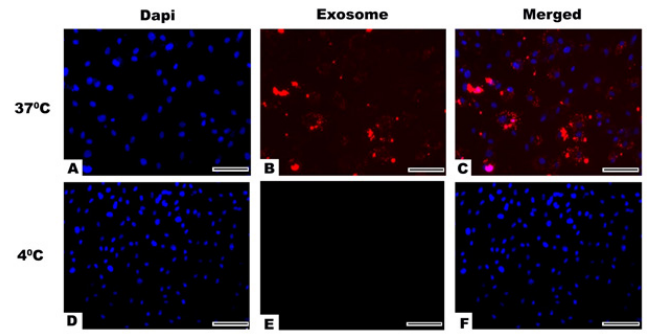

Figure 4. Fluorescence microscopy analysis of EV uptake by cells at different temperatures. Exosome uptake by cells was examined to show the ability of exosomes to enter the cells. Cells kept at 4°C or 37°C were incubated with PKH26-labeled EVs for 1.5 hours. In images of MSCs incubated at different temperatures, much more fluorescence was observed in cells incubated at 37°C, as shown in **Figures 4A, B & C,** than those at 4°C, as shown in **Figures 4D, E & F** demonstrating that EVs entered into the cells. The experiments were performed twice. In each experiment, cells on four cover slips (placed in 24-well plates) were treated under a particular condition. These are representative images. **(H & E stain, magnification power = x400, scale bar = 50 µm)**.

sue of all investigated groups are summarized in Table 2. MDA was markedly increased, while TAC was substantially reduced in the diabetic nephropathy group compared to normal rats ($P < 0.001$). The undesirable elevation in pancreatic MDA level and reductions in pancreatic TAC level were markedly ameliorated in the group co-administered *Balanites aegyptiaca* with MSCs or exosomes than in diabetic nephropathy rats ($P < 0.001$).

Histopathology

Normal pancreatic parenchyma and lobules with normal pancreatic acini and acinar cells were observed in the pancreas of normal rats (arrows) (HE X400) (lesion score: 0) (Figure 5A). Conversely, the positive control group revealed massive cortical necrosis; necrosis and disintegration of the glomerular tuft (arrow) led to the widening of the capsular spaces (*), (HE X 400) (lesion score: ++++) (Figure 5B). Diabetic nephropathy rats treated with both *Balanites aegyptiaca* and exosomes revealed the best results (Figure 5F). In contrast, other groups gradually revealed some improvement in pancreatic tissue according to the lesion score: (Figures 5C- 5G).

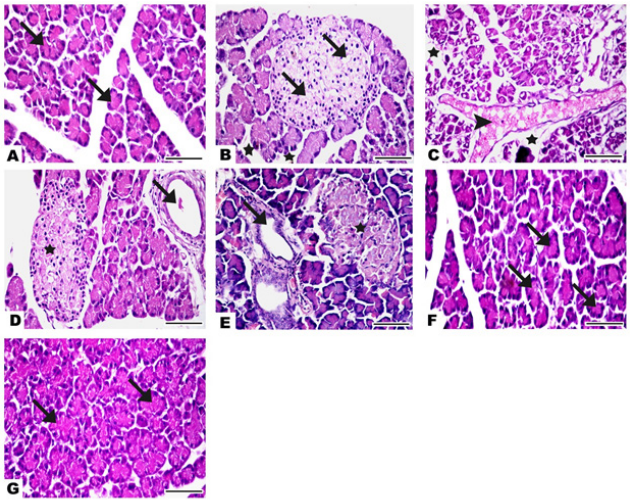

Figure 5. Photomicrographs of pancreatic tissue of all groups investigated: (**A**) Pancreas from the negative control group revealed normal pancreatic parenchyma; noted the normal pancreatic lobules with normal pancreatic acini and acinar cells (arrows) (lesion score 0). (**B**) The pancreas section from the positive control group revealed massive cortical necrosis; noted the necrosis and disintegration of glomerular tufts (arrow) leading to the widening of the capsular spaces (*) (lesion score ++++). (**C**) The pancreas from the *Balanites* treated group revealed dilatation and congestion in the interlobular and intralobular blood vessels (arrowhead) together with intralobular edema (*) (lesion score +++). (**D**) The pancreas from the *Balanites* + MSC treated group showed dilatation in the pancreatic duct (arrow) and hyperplasia in the pancreatic Langerhans islets with nuclei and normal cells (*) (lesion score ++). (**E**) The pancreas from the MSC-treated group revealed dilatation in the pancreatic duct (arrow) and hyperplasia in the pancreatic Langerhans islets with nuclei and normal cells (*) (lesion score +++). (**F**) The pancreas from the *Balanites* + exosome treated group revealed normal pancreatic parenchyma; the normal pancreatic lobules with normal pancreatic acini and acinar cells (arrows) (lesion score 0). (**G**) The exosome-treated group's pancreas revealed normal pancreatic parenchyma; noted the normal pancreatic lobules with normal pancreatic acini and acinar cells (arrows) (lesion score 0). **(H & E stain, magnification power = x400, scale bar = 50 µm)**.

Discussion

There has recently been an increase in concern regarding the development of exosomes. Exosomes are natural nano-scale particles that possess numerous benefits.

Table 2. Effect of exosome, MSCs, and *Balanites aegyptiacae* on MDA and TAC in pancreatic tissue of all investigated groups.

Groups	MDA(nmol/g tissue)	% change	TAC (mM/L)	% change	P Value
Negative control group	108±2.1^{c}	---	65.8±0.61^{c}	---	
Positive control group	179.8±5.2***	66.48%	23.2±0.82***	-64.74%	
Balanites treated group	113.4±1.4^{c}	-36.92%	38.8±0.24***^{c}	67.24%	
MSCS treated group	156.4±4.5***^{a}	-13.01%	33.2±0.24***^{c}	43.10%	
Exosome-treated group	157.2±2.4***^{a}	-12.56%	47±0.86***^{c}	102.58%	
Balanites + MSCs treated group	82.4±2.1***^{c}	-54.17%	54.6±0.49***^{c}	135.34%	< 0.001
Balanites + exosomes treated group	89.8±3.5*^{c}	-50.05%	80±2.8*^{c}	244.82%	

Values are expressed as mean ± SEM, n = 10. Various superscript letters for values represent significant differences ($P<0.05$). * $P< 0.05$ compared to control group, ** $P< 0.01$, *** $P< 0.001$ compared to control group. $^{a}P< 0.05$, $^{b}P< 0.01$, $^{c}P< 0.001$ compared to positive control group. The percentage of change of positive control was calculated according to the negative control.

In the last decade, exosome-related basic research and clinical studies have penetrated numerous medical specialties (29). Almost all cells can secrete exosomes, and different exosome types have different functions. A significant subset of stem cells known as MSCs has attracted attention as a possible starting point for tissue engineering, cell therapy, and regenerative medicine studies. Therefore, research based on MSC exosomes offers a lot of significance (30). In addition to producing significant amounts of anti-apoptotic substances such as insulin growth promoter (IGF-I), anti-inflammatory substances, interleukin (IL-6), and interleukin-1 receptor antagonist (IL-1Ra), MSCs also function in a paracrine manner in which they create unique exosomes and microvesicles (31).

Studies have demonstrated that MSCs function via their paracrine action, or how secreted EVs function. In particular, MSCs produce exosomes that may have a definite therapeutic effect in disorders characterized by inflammation or tissue damage (32). Many exosome isolation techniques have limitations, including exosome preparation on a large scale, reduced scalability, poor reproducibility, expensive supplies and reagents, limitations on the capacity to create significant amounts of exosomes, and low recovery (33). Furthermore, differential centrifugation is the approach for exosomes most frequently utilized among all these techniques because large-scale conditioned medium handling for exosome isolation is inexpensive and simple (34). In the current investigation, we attempted to identify exosome morphology, recognize exosomes secreted into an MSC-conditioned cell culture medium, and fully characterize those exosomes. We purified exosomes from MSCs' conditioned medium using ultracentrifugation and used a BCA assay kit to perform a colorimetric analysis.

The current study's findings are inconsistent with a prior study (35), which demonstrated that exosomes produced by ultracentrifugation from 1 million cells had a yield of 1.5×10^8 particles and a relatively low protein concentration level of 3 μg for their function in Alzheimer's disease. Isolated vesicles were primarily 175 nm in size. Nevertheless, another study (33) demonstrated that crude exosomes extracted by ultracentrifugation might be further purified on a sucrose gradient, thereby removing potential impurities.

In general, the presence of exosomes was assessed using Western blot analysis, TEM, and NTA. Nanoparticle tracking analysis, which measures the yield of exosomes and size, is one of the fundamental characterization methods used for exosome detection. Western blotting can also be utilized to determine exosome-specific markers. Exosome identification markers include TSG101, Alix, syntenin-1, Hsp90, Hsp70, flotillin-1, LAMP2, cofilin, and Tetraspanins (CD9, CD63, and CD81) (36). Exosomes derived from BMSCs are homogeneous in size with a 30 to 100 nm diameter range and have a cup-shaped morphology with definite and visible boundaries (37). Our TEM observation demonstrated the presence of nano-vesicles, and the sizes of individual EVs varied according to electron microscopy using ranges of average diameter from 30-150 nm. The center of exosomal vesicles generally has a divot, probably because the sample preparation for TEM requires drying.

The total concentration and size of vesicles can be determined using NTA. However, it is insufficient to distinguish between biological and synthetic nanoparticles (38). In addition to determining the hydrodynamic size of undamaged vesicles, NTA eliminates the need for sample preparation that can alter exosome morphology. By quantifying the difference in concentration between healthy and diseased/inflammatory conditions, it may be possible to more fully utilize NTA's ability to predict the size and concentration of EVs as well as their subtypes (exosomes) (39). According to our NTA findings, preparations with sharper size distribution curves were more homogeneous.

Since exosomes contain unique markers from their parent cell, they might have characteristics similar to those originating from them. These markers are utilized for therapeutic and diagnostic purposes, yet they have proven to be a double-edged sword (40). Due to its simplicity, accessibility, and capacity to identify both exosomal surface proteins and interior proteins, Western blotting is the method most frequently employed to detect target proteins linked with EVs (41). Tetraspanins CD9, CD63, and CD81 are surface markers prevalent in both MVs and exosomes, complicating their usage as exosome biomarkers (42).

The samples isolated using ultracentrifugation techniques were significantly enriched for exosome markers. All exosome preparations contained both the transmembrane protein (CD63) and the cytosolic protein (TSG101). On the contrary, the other transmembrane protein (CD9) was only detected in exosomes isolated using ultracentrifugation. It was not present in exosomes acquired through the Total Exosomes Isolation Reagent (TEI) and Exo-Quick kits (43). It is preferable to compare the composition of EVs to that of the secreting cells. Exosomes obtained using ultracentrifugation were more enriched in EV components than the originating cells (CD9 and TSG101) or even more enriched (CD63 and CD9). The weak bands were observed in cell culture media, indicating that the supernatant contained substantial amounts of the remaining EVs 70 minutes after ultracentrifugation (44).

After injection, STZ quickly reaches the pancreatic beta cells and breaks DNA strands (45,46). By elevating the production of H_2O_2, STZ causes the production of ROS, which in turn causes DNA fragmentation in the pancreatic β-cell islets (47). Blood glucose levels rise in conjunction with changes to the damaged pancreatic islets led on by the onset of diabetes (48). Nicotinamide lessens the severity of diabetes in rats induced by STZ owing to its antioxidant action (49,50). As a result, a type II diabetes model produced by STZ-nicotinamide was used for this investigation. Excessive ROS generation can be stimulated by a high glucose environment and lead to DN (51). Malondialdehyde, a byproduct of the lipid peroxidation reaction, can be utilized as a biomarker to determine levels of oxidative stress. MDA is increased in conditions that cause oxidative stress, such as diabetes mellitus (52).

This study revealed that the combination of *Balanites aegyptiaca* with exosomes had significantly higher nephroprotective and anti-diabetic effects than either alone. To our knowledge, this is the first report to investigate this combination's nephroprotective and anti-diabetic properties. Malondialdehyde concentrations in the pancreatic tissue of diabetic nephropathy rats were significantly higher than those of normal rats. At the same time, groups co-administered *Balanites aegyptiaca* with exosomes or MSCs demonstrated a substantial decrease in malondialdehyde concentrations compared to diabetic nephropathy rats. The levels of TAC in the pancreatic tissue of the diabetic

nephropathy rats were significantly decreased compared to normal rats.

In contrast, groups co-administered *Balanites aegyptiaca* with exosome or MSCs demonstrated a considerable increase in TAC levels compared to diabetic nephropathy rats. The fruit mesocarp of *Balanites aegyptiaca* is frequently utilized as an oral diabetic treatment in Egyptian folk medicine (53). *Balanites aegyptiaca* extract has a hypoglycemic action mediated by insulin-mimetic action (54), enhanced sensitivity for insulin receptors, potentiation and stimulation of insulin secretion (55), inhibition of intestinal glucosidase activity, acceleration of glucose metabolism, suppression of hepatic gluconeogenesis, and improved hepatic glycogen storage (56).

Since only 1% of MSCs can access the desired tissue, and data suggest that MSCs developed into target cells are deficient, MSCs now use paracrine activity rather than proliferative potential to heal damaged tissue (57). One of the most crucial methods for paracrine regulation is using exosomes. Prior research revealed that exosomes are superior MSC replacements and are crucial for repairing oxidative damage to the liver and repairing injured organs or tissues by releasing bioactive molecules like Wnt4 (58). Exosomes secreted by bone marrow stem cells can alleviate the nephropathy and cognitive impairment caused by diabetes (59). MSCs may repair cisplatin-damaged proximal tubular cells owing to the simultaneous trophic action of insulin-like growth factor 1 secreted by bone marrow-MSCs and the transmission of the mRNA of the appropriate IGF-1 receptor using exosomes (60). MSC-ex may be necessary for preventing autoimmune targeting of the pancreatic islets in T1DM patients and slowing the disease progression (61).

The current study revealed that ultracentrifugation is the most popular technique for isolating exosomes. Exosomes may be nanoparticles that contain bioactive molecules that reflect an individual's physiological status, regulate metabolism, and repair impaired tissues. In addition, it demonstrated that *Balanites aegyptiaca* and exosomes have synergistic benefits for each other and have more potent renoprotective and anti-diabetic effects in rats with diabetic nephropathy.

Authors' contributions

All authors participated in the design, interpretation of the studies, data analysis, and manuscript review.

Declaration of conflicting interests

The authors declare no potential conflicts of interest concerning this article's research, authorship, and/or publication.

Funding

The author(s) received no financial support for this article's research, authorship, and/or publication.

References

1. Théry C, Zitvogel L, Amigorena S. Exosomes: Composition, biogenesis and function. Nat Rev Immunol 2002; 2: 569–579.
2. Lener T, Gimona M, Aigner L, *et al.* Applying extracellular vesicles based therapeutics in clinical trials - An ISEV position paper. J Extracell Vesicles 2015; 4(1): 30087.
3. Skotland T, Sandvig K, Llorente A. Lipids in exosomes: Current knowledge and the way forward. Prog Lipid Res 2017; 66: 30–41.
4. Li P, Kaslan M, Lee SH, Yao J, Gao Z. Progress in exosome isolation techniques. Theranostics 2017; 7: 789–804.
5. Raposo G, Stoorvogel W. Extracellular vesicles: Exosomes, microvesicles, and friends. J Cell Biol 2013; 200: 373–383.
6. Lai RC, Tan SS, Yeo RWY, *et al.* MSC secretes at least 3 EV types each with a unique permutation of membrane lipid, protein and RNA. J Extracell Vesicles 2016; 5 (1): 29828.
7. Colombo M, Raposo G, Théry C. Biogenesis, secretion, and intercellular interactions of exosomes and other extracellular vesicles. Annu Rev Cell Dev Biol 2014; 30: 255–289.
8. Andreu Z, Yáñez-Mó M. Tetraspanins in extracellular vesicle formation and function. Front Immunol 2014; 5: 1–12.
9. Kalluri R. The biology and function of exosomes in cancer. J Clin Invest 2016; 126: 1208–1215.
10. Lai RC, Arslan F, Lee MM, *et al.* Exosome secreted by MSC reduces myocardial ischemia/reperfusion injury. Stem Cell Res 2010; 4: 214–222.
11. Huang L, Ma W, Ma Y, Feng D, Chen H, Cai B. Exosomes in mesenchymal stem cells, a new therapeutic strategy for cardiovascular diseases? Int J Biol Sci 2015; 11: 238–245.
12. Carlson ED, Gan R, Hodgman CE, Jewett MC. Cell-free protein synthesis: Applications come of age. Biotechnol Adv 2012; 30: 1185–1194.
13. Gurunathan S, Kang M, Jeyaraj M, Qasim M, Kim J. Function, and Multifarious Therapeutic Approaches of Exosomes. Cells 2019; 8: 307.
14. Bruno S, Grange C, Collino F, *et al*. Microvesicles derived from mesenchymal stem cells enhance survival in a lethal model of acute kidney injury. PLoS One 2012; 7(3): e33115.
15. Théry C, Clayton A, Amigorena S, Raposo G. Isolation and Characterization of Exosomes from Cell Culture Supernatants. Curr Protoc Cell Biol 2006; 30 (1): 3-22.
16. Li L, Piontek KB, Kumbhari V, Ishida M, Selaru FM. Isolation and profiling of microRNA-containing exosomes from human bile. J Vis Exp 2016; 112: e54036.
17. Cheng H, Fang H, Xu RD, Fu MQ, Chen L, Song XY, Qian JY, Zou YZ, Ma JY, Ge JB. Development of a rinsing separation method for exosome isolation and comparison to conventional methods. Eur Rev Med Pharmacol Sci. 2019; 23(12): 5074-5083.
18. Lange-Consiglio A, Perrini C, Albini G, *et al*. Oviductal microvesicles and their effect on in vitro maturation of canine oocytes. Reproduction 2017; 154: 167–180.
19. El Deib MM, Ali HA. Molecular investigation of anti-diabetic effect of balanites aegyptiaca fruits in streptozotocin-induced diabetic rats. Slov Vet Res 2018; 55: 137–145.
20. Punitha ISR, Rajendran K, Shirwaikar A, Shirwaikar A. Alcoholic stem extract of Coscinium fenestratum regulates carbohydrate metabolism and improves antioxidant status in streptozotocin-nicotinamide induced diabetic rats. Evidence-based Complement Altern Med 2005; 2: 375–381.
21. Ebrahim N, Ahmed IA, Hussien NI, *et al.* Mesenchymal stem cell-derived exosomes ameliorated diabetic nephropathy by autophagy induction through the mTOR signaling pathway. Cells 2018; 7: 1–26.
22. Nagaishi K, Mizue Y, Chikenji T, Otani M, Nakano M, Konari N, Fujimiya M. Mesenchymal stem cell therapy ameliorates diabetic nephropathy via the paracrine effect of renal trophic factors including exosomes. Sci Rep 2016; 6: 1–16.
23. Yang J, Liu XX, Fan H, *et al*. Extracellular vesicles derived from bone marrow mesenchymal stem cells protect against experimental colitis via attenuating colon inflammation, oxidative stress and apoptosis. PLoS One 2015; 10: 1–19.
24. Ohkawa H, Ohishi N, Yagi K. Assay for lipid peroxides in animal tissues by thiobarbituric acid reaction. Anal Biochem 1979; 95:

351–358.
25. Koracevic D, Koracevic G, Djordjevic V, Andrejevic S, Cosic V. Method for the measurement of antioxidant activity in human fluids. J Clin Pathol 2001; 54: 356–361.
26. Palipoch S, Punsawad C. Biochemical and histological study of rat liver and kidney injury induced by cisplatin. J Toxicol Pathol 2013; 26: 293–299.
27. Houghton DC, Plamp CE, DeFehr JM, Bennett WM, Porter G, Gilbert D. Gentamicin and tobramycin nephrotoxicity. A morphologic and functional comparison in the rat. Am J Pathol 1978; 93: 137–152.
28. Abu-Bader SH. Using statistical methods in social science research: with a complete SPSS guide. 3rd ed. Oxford: Oxford University Press 2021; pp.297–302.
29. Bebelman MP, Bun P, Huveneers S, van Niel G, Pegtel DM, Verweij FJ. Real-time imaging of multivesicular body–plasma membrane fusion to quantify exosome release from single cells. Nat Protoc 2020; 15: 102–121.
30. Riazifar M, Mohammadi MR, Pone EJ, *et al*. Stem Cell-Derived Exosomes as Nanotherapeutics for Autoimmune and Neurodegenerative Disorders. ACS Nano 2019; 13: 6670–6688.
31. Nabil A, Uto K, Zahran F, *et al*. The potential safe antifibrotic effect of stem cell conditioned medium and nilotinib combined therapy by selective elimination of rat activated HSCS. Biomed Res Int 2021; 2021.
32. Wei W, Ao Q, Wang X, Cao Y, Liu Y, Zheng SG, Tian X. Mesenchymal Stem Cell–Derived Exosomes: A Promising Biological Tool in Nanomedicine. Front Pharmacol 2021; 11: 1–13.
33. Alexander RP, Chiou N-T, Ansel KM. Improved exosome isolation by sucrose gradient fractionation of ultracentrifuged crude exosome pellets. Protoc Exch 2016; 1–4.
34. Lobb RJ, Becker M, Wen SW, Wong CSF, Wiegmans AP, Leimgruber A, Möller A. Optimized exosome isolation protocol for cell culture supernatant and human plasma. J Extracell Vesicles 2015; 4(1): 27031.
35. Katsuda T, Tsuchiya R, Kosaka N, *et al*. Human adipose tissue-derived mesenchymal stem cells secrete functional neprilysin-bound exosomes. Sci Rep 2013; 3(1): 1–11.
36. Kowal J, Arras G, Colombo M, *et al*. Proteomic comparison defines novel markers to characterize heterogeneous populations of extracellular vesicle subtypes. Proc Natl Acad Sci U S A 2016; 113(8): E968–E977.
37. Tang Y, Zhou Y, Li HJ. Advances in mesenchymal stem cell exosomes: a review. Stem Cell Res Ther 2021; 12(1): 1–12.
38. Gercel-Taylor C, Atay S, Tullis RH, Kesimer M, Taylor DD. Nanoparticle analysis of circulating cell-derived vesicles in ovarian cancer patients. Anal Biochem 2012; 428: 44–53.
39. Chopra N, Dutt Arya B, Jain N, Yadav P, Wajid S, Singh SP, Choudhury S. Biophysical Characterization and Drug Delivery Potential of Exosomes from Human Wharton's Jelly-Derived Mesenchymal Stem Cells. ACS Omega 2019; 4: 13143–13152.
40. Mendt M, Kamerkar S, Sugimoto H, *et al*. Generation and testing of clinical-grade exosomes for pancreatic cancer. JCI insight 2018; 3: 1–22.
41. Di Bella MA. Overview and Update on Extracellular Vesicles: Considerations on Exosomes and Their Application in Modern Medicine. Biology (Basel) 2022; 11(6): 804.
42. Wu SC, Kuo PJ, Rau CS, *et al*. Subpopulations of exosomes purified via different exosomal markers carry different microrna contents. Int J Med Sci 2021; 18(4): 1058–1066.
43. Lötvall J, Hill AF, Hochberg F, *et al*. Minimal experimental requirements for definition of extracellular vesicles and their functions: A position statement from the International Society for Extracellular Vesicles. J Extracell Vesicles 2014; 3: 1–6.
44. Cvjetkovic A, Lötvall J, Lässer C. The influence of rotor type and centrifugation time on the yield and purity of extracellular vesicles. J Extracell Vesicles 2014; 3: 1–11.
45. Shivavedi N, Charan Tej GNV, Neogi K, Nayak PK. Ascorbic acid therapy: A potential strategy against comorbid depression-like behavior in streptozotocin-nicotinamide-induced diabetic rats. Biomed Pharmacother 2019; 109: 351–359.
46. Mali KK, Ligade SS, Dias RJ. Delaying effect of polyherbal formulation on cataract in STZ-NIC-induced diabetic wistar rats. Indian J Pharm Sci 2019; 81: 415–423.
47. Bennett RA, Pegg AE. Alkylation of DNA in rat tissues following administration of streptozotocin. Cancer Res 1981; 41(7):2786-2790.
48. Elkotby D, Hassan AK, Emad R, Bahgat I. Histological Changes in Islets of Langerhans of Pancreas in Alloxan-Induced Diabetic Rats Following Egyptian Honey Bee Venom Treatments. Int J Pure Appl Zool 2018; 6: 1–6.
49. Yamada K, Nonaka K, Hanafusa T, Miyazaki A, Toyoshima H, Tarui S. Preventive and therapeutic effects of large-dose nicotinamide injections on diabetes associated with insulitis: an observation in nonobese diabetic (NOD) mice. Diabetes 1982; 31(9): 749–753.
50. Cruz PL, Moraes-Silva IC, Ribeiro AA, *et al*. Nicotinamide attenuates streptozotocin-induced diabetes complications and increases survival rate in rats: role of autonomic nervous system. BMC Endocr Disord 2021; 21: 1–10.
51. Ha H, Hi Bahl Lee. Reactive oxygen species as glucose signaling molecules in mesangial cells cultured under high glucose. Kidney Int Suppl 2000; 58: 19–25.
52. Tripathi P, Verma MK, Tripathi SS, Singh SP. Comparative Study of Malondialdehyde and Vitamin C in Type 2 Diabetes Mellitus and Non Diabetic Individuals. Int J Life Sci Sci Res 2016; 2: 31–36.
53. Gnoula C, Mégalizzi V, De Nève N, *et al*. Balanitin-6 and -7: Diosgenyl saponins isolated from Balanites aegyptiaca Del. display significant anti-tumor activity in vitro and in vivo. Int J Oncol 2008; 32: 5–15.
54. Motaal AA, Shaker S, Haddad PS. Antidiabetic activity of standardized extracts of Balanites aegyptiaca fruits using cell-based bioassays. Pharmacogn J 2012; 4: 20–24.
55. Abde-Moneim A. Effect of some medicinal plants and gliclazide on insulin release in vitro. JOURNAL-EGYPTIAN Ger Soc Zool 1998; 25: 423–445.
56. Gad MZ, El-Sawalhi MM, Ismail MF, El-Tanbouly ND. Biochemical study of the anti-diabetic action of the egyptian plants fenugreek and balanites. Mol Cell Biochem 2006; 281: 173–183.
57. Si Y, Zhao Y, Hao J, *et al*. Infusion of mesenchymal stem cells ameliorates hyperglycemia in type 2 diabetic rats: Identification of a novel role in improving insulin sensitivity. Diabetes 2012; 61: 1616–1625.
58. Zhang B, Wang M, Gong A, *et al*. HucMSc-exosome mediated-Wnt4 signaling is required for cutaneous wound healing. Stem Cells 2015; 33: 2158–2168.
59. Nagaishi K, Mizue Y, Chikenji T, *et al*. Umbilical cord extracts improve diabetic abnormalities in bone marrow-derived mesenchymal stem cells and increase their therapeutic effects on diabetic nephropathy. Sci Rep 2017; 7: 1–17.
60. Tomasoni S, Longaretti L, Rota C, *et al*. Transfer of growth factor receptor mRNA via exosomes unravels the regenerative effect of mesenchymal stem cells. Stem Cells Dev 2013; 22: 772–780.
61. Bu N, Wu HQ, Zhang GL, *et al*. Immature dendritic cell exosomes suppress experimental autoimmune myasthenia gravis. J Neuroimmunol 2015; 285: 71–75. veux je te depose ton